



Title	First principles calculation of ac conductance for AI-BDT-AI and AI-Cn-AI systems
Author(s)	Zhuang, JN; Zhang, L; Wang, J
Citation	AIP Advances, 2011, v. 1 n. 4, article no. 042180, p. 042180-1-042180-13
Issued Date	2011
URL	http://hdl.handle.net/10722/159787
Rights	AIP Advances. Copyright © American Institute of Physics.

First principles calculation of ac conductance for Al-BDT-Al and Al-Cn-Al systems

Jia-Ning Zhuang, Lei Zhang, and Jian Wang

Citation: *AIP Advances* **1**, 042180 (2011); doi: 10.1063/1.3673566

View online: <http://dx.doi.org/10.1063/1.3673566>

View Table of Contents: <http://aipadvances.aip.org/resource/1/AAIDBI/v1/i4>

Published by the [American Institute of Physics](http://www.aip.org).

Related Articles

The effects of Bi alloying in Cu delafossites: A density functional theory study
J. Appl. Phys. **109**, 113710 (2011)

18th Ural International Winter School on the Physics of Semiconductors
Low Temp. Phys. **37**, 177 (2011)

Rapid consolidation of powdered materials by induction hot pressing
Rev. Sci. Instrum. **82**, 025104 (2011)

A study on the modulation of the electrical transport by mechanical straining of individual titanium dioxide nanotube
Appl. Phys. Lett. **97**, 072107 (2010)

Modeling of transient electrical characteristics for granular semiconductors
J. Appl. Phys. **108**, 034511 (2010)

Additional information on AIP Advances

Journal Homepage: <http://aipadvances.aip.org>

Journal Information: <http://aipadvances.aip.org/about/journal>

Top downloads: http://aipadvances.aip.org/most_downloaded

Information for Authors: <http://aipadvances.aip.org/authors>

ADVERTISEMENT



AIPAdvances

Now Indexed in Thomson Reuters Databases

Explore AIP's open access journal:

- Rapid publication
- Article-level metrics
- Post-publication rating and commenting

First principles calculation of ac conductance for Al-BDT-Al and Al-C_n-Al systems

Jia-Ning Zhuang, Lei Zhang, and Jian Wang^a

Department of Physics and the Center of Theoretical and Computational Physics, The University of Hong Kong, Pokfulam Road, Hong Kong, China

(Received 20 September 2011; accepted 1 December 2011; published online 15 December 2011)

We perform first-principles calculation to investigate the dynamic conductance of atomic wires of the benzenedithiol (BDT) as well as carbon chains with different length in contact with two Al(100) electrodes (Al-C_n-Al). Our calculation is based on the combination of the non-equilibrium Green's function and the density functional theory. For ac conductance, there are two theories that ensures the current conservation: (1). the global formula which is a phenomenological theory that partitions the total displacement current into each leads so that the current is conserved. (2). the local formula which is a microscopic theory that includes Coulomb interaction explicitly so that the current is conserved automatically. In this work, we use the local formula to calculate the dynamic conductance, especially the emittance. We give a detailed comparison and analysis for the results obtained from two theories. Our numerical results show that the global formula overestimates the emittance by two orders of magnitude. We also obtain an inequality showing that the emittance from global formula is greater than that from local formula for real atomic structures. For Al-C_n-Al structures, the oscillatory behavior as the number of carbon chain *N* varies from even to odd remains unchanged when local formula is used. However, the prediction of local formula gives rise to opposite response when *N* is odd (inductive-like) as compared with that of global formula. Therefore, one should use the local formula for an accurate description of ac transport in nanoscale structures. In addition, the 'size effect' of the ac emittance is analyzed and can be understood by the kinetic inductance. Since numerical calculation using the global formula can be performed in orbital space while the local formula can only be used in real space, our numerical results indicate that the calculation using the local formula is extremely computational demanding. *Copyright 2011 Author(s). This article is distributed under a Creative Commons Attribution 3.0 Unported License.* [doi:10.1063/1.3673566]

I. INTRODUCTION

Quantum transport in nanostructures under ac bias has been the subject of intense studies both experimentally and theoretically.¹⁻¹² Ac response is of fundamental interest because it can probe the charge distribution and the dynamics of the system. In addition, the frequency introduces another energy scale into the problem. So far, ac has been studied for a variety of systems including normal quantum dot systems^{1,3,8} as well as normal superconducting hybrid system.⁶ When the strongly electron-electron interaction is included, an exact solution of ac has been obtained in the Kondo regime.⁵ In addition to frequency-dependent current, transient current⁴ and photon-assisted shot noise^{2,7} have also been investigated. At low frequencies, the dynamic response of a quantum capacitor can be described by a quantum capacitance in series with a charge-relaxation resistance.⁹ For a conductor that allows single-channel transmission, the charge-relaxation resistance

^aEmail: jianwang@hku.hk



was predicted to be half of the resistance quanta^{9,10} and was confirmed experimentally.¹¹ Due to the existence of quantum inductance, the current accumulates a phase and lags behind the voltage leading to a negative capacitance.¹²

In the theoretical treatment, the current is usually defined in terms of conduction current, i.e., $I_\alpha^c = dq_\alpha/dt$, where q_α is the charge flowing into the α lead. From the continuity equation $\sum_\alpha I_\alpha^c + dQ/dt = 0$ we see that the conduction current I_α^c is a conserved quantity only in the case of dc. Under the ac bias, however, the conduction current is not a conserved quantity anymore. The displacement current I_α^d due to the charge pileup dQ/dt inside the scattering region becomes important and must be considered. The problem of current conserving can be solved by partitioning the total displacement current $\sum_\alpha I_\alpha^d = dQ/dt$ into each lead giving rise to a conserved total current $I_\alpha = I_\alpha^c + I_\alpha^d$. The current partition at small bias was achieved by Büttiker *et al.*¹³ using the scattering matrix approach, and was extended to the situation far from equilibrium using non-equilibrium Green's function (NEGF) method.¹⁴ This formalism ensures both the current conserving condition as well as the gauge-invariant condition which says that the current of a multi-probe system remains the same if all the bias are shifted by the same amount. Therefore, this formula has been used in most of the recent *ab-initio* calculations for real atomic structures,¹⁵⁻¹⁷ and some interesting results have been obtained. Since the Coulomb interaction giving rise to the displacement current is not considered explicitly, the above formalism is phenomenological in nature. In the present paper we call this formula the 'global' formula since the displacement current is expressed in terms of global quantities such as the scattering matrix.

Despite its success, it is pointed out that in the global formula, the dynamic conductance at general frequency $G_{\alpha\beta}(\omega)$ was only treated at level of current partition.¹⁸ The reason is that only a formal definition of $G_{\alpha\beta}$ was presented in the linear-response theory¹⁹ and the Coulomb interaction was only implicitly introduced. In order to fill this gap, a microscopic theory for ac transport was developed by using the non-equilibrium Green's function theory¹⁸ (in the present paper we call this formula 'local' because the displacement is considered in every point in real space). In this new theory, the Coulomb interaction treated at Hartree level is taken into account explicitly, and the predicted ac current also satisfies the current conserving and gauge-invariant conditions. Because the global and the local formulae are expressed in NEGF, both can be used to combine with the density-functional theory(DFT)²⁰ to perform *ab initio* calculation for realistic atomic structures.

In the present paper, we investigate the frequency dependent conductance of nano-devices using NEGF+DFT method. In particular, we compare dynamic conductance especially the ac emittance calculated from the global and the local formulae. We find that in general the global formula overestimate the emittance by two orders of magnitude. For the atomic structure of carbon chain coupled with two Al leads Al-C_n-Al, our results show that the qualitative features are the same for oscillatory behavior using global and local formulae. However, they predict different dynamical response behavior of the system when the number of carbon chain is odd. The rest of the paper is organized as follows. In Sec. II, we briefly review the global and the local formula for the dynamical conductance and the ac emittance. In Sec. III, we compare the numerical results obtained by both formulae, and make some analysis. A 'size effect' of the numerical result is reported in Sec. IV along with a brief summary, and the conclusions are given in Sec. V. The atomic unit is used throughout this paper unless otherwise stated.

II. REVIEW OF TWO DIFFERENT FORMULAE

In this section, we present a review of global and the local formulae for the dynamical conductance as well as the ac emittance. We avoid going through every detail of the derivation, but only stress some of the key points that worth noticing.

A. Global formula

The global formula for the ac conductance was firstly proposed by Büttiker *et al.*¹³ using the scattering matrix approach, and reformulated by Wang *et al.*¹⁴ using NEGF. Following the procedure of the latter work, the starting point is the expression of the *particle current* or conduction current^{4,21}

I_α^c inside each probe. In the small bias limit, the corresponding conductance of this particle current reads

$$G_{\alpha\beta}^c(\omega) = - \int \frac{dE}{2\pi} \frac{f - \bar{f}}{\omega} \text{Tr}[-i(\bar{G}^r - G^a)\Gamma_\alpha \delta_{\alpha\beta} + \bar{G}^r \Gamma_\beta G^a \Gamma_\alpha], \quad (1)$$

where G^r is the equilibrium Green's function and $\bar{G}^r = G^r(E + \omega)$; Γ_α is the linewidth function defined as $\Gamma_\alpha = i[\Sigma_\alpha^r - \Sigma_\alpha^a]$ (Σ_α^r and Σ_α^a are retarded and advanced self-energy of lead α) describing the coupling strength between the α lead and the scattering region; f is the Fermi distribution function and $\bar{f} = f(E + \omega)$. We point out that in the expression given above, the wideband approximation has been used so that terms involving $\partial_E \Sigma^{r,a}$ are neglected.

Due to the charge accumulation, the particle conductance does not conserve the current and violates gauge invariance. That the particle current alone is not a conserved quantity means that $\sum_\alpha G_{\alpha\beta}^c \neq 0$, or equivalently, I_α^c do not sum up to zero. Their sum is equal to the time rate of change of charge Q stored inside the device dQ/dt . In the frequency space, we have:

$$\sum_\alpha I_\alpha^c(\omega) = i\omega Q(\omega). \quad (2)$$

In order to solve the current conserving problem, one can partition this total displacement current into each leads⁹ by using $i\omega Q(\omega) = \sum_\beta G_\beta^d$, where

$$G_\beta^d = -i \int \frac{dE}{2\pi} \text{Tr}[\bar{G}^r \Gamma_\beta G^a (f - \bar{f})] \quad (3)$$

can be viewed as the displacement current, up to a multiple coefficient. Next, by carefully enforcing the gauge-invariant condition $\sum_\beta G_{\alpha\beta} = 0$, one obtains the final expression of the ac conductance:

$$G_{\alpha\beta}(\omega) = G_{\alpha\beta}^c(\omega) - G_\beta^d(\omega) \frac{\sum_\gamma G_{\alpha\gamma}^c(\omega)}{\sum_\gamma G_\gamma^d(\omega)}. \quad (4)$$

As we mentioned before, Eq.(4) is called the global formula for ac conductance in the present paper. All the first principles quantum transport calculations for ac conductance through atomic junctions are based on this formula. However, the main problem of the global formula is that the Coulomb potential is not explicitly dealt with, but only implicitly introduced by enforcing the gauge-invariant condition. Both current-conserving and gauge-invariant are just necessary conditions, and we indeed have other choices. The *local formula* presented in the next subsection is an example. This formula is a microscopic theory and the Coulomb potential is taken into account explicitly.

B. Local formula

The *local formula* was derived in detail in Ref. 18. In the wide-band limit, the frequency-dependent ac conductance can be written as¹⁸

$$G_{\alpha\beta}(\omega) = G_{\alpha\beta}^c - i\omega \int \frac{dE}{2\pi} \text{Tr}[\Gamma_\alpha \bar{G}^r u_\beta(\omega) G^a] \frac{f - \bar{f}}{\omega}. \quad (5)$$

Here u_α is the characteristic potential that satisfies the following Poisson like equation

$$\nabla^2 u_\alpha(\omega, x) = -4\pi \frac{dn_\alpha(\omega, x)}{dE} + 4\pi \frac{dn(\omega, x)}{dE} u_\alpha(\omega, x), \quad (6)$$

where we have used the Thomas-Fermi approximation⁹ and the frequency-dependent injectivity $dn_\alpha(\omega, x)/dE$ is defined as^{10,12}

$$\frac{dn_\alpha(\omega, x)}{dE} = \int \frac{dE}{2\pi} \frac{f - \bar{f}}{\omega} [\bar{G}_0^r \Gamma_\alpha G_0^a]_{xx}, \quad (7)$$

In principle, Eq.(5) can be used in the *ab initio* transport calculations for the atomic structures, but we have to solve several Poisson equations with complicated boundary conditions to get $u_\beta(\omega)$ for each lead. To further simplify Eq.(5), we use quasi-neutrality approximation, i.e. $\nabla^2 u_\alpha(\omega, x) = 0$, then the dynamic conductance becomes

$$G_{\alpha\beta}(\omega) = G_{\alpha\beta}^c(\omega) - i\omega \text{Tr} \left[\frac{d\bar{n}_\alpha(\omega, x)}{dE} \frac{dn_\beta(\omega, x)}{dE} / \frac{dn(\omega, x)}{dE} \right], \quad (8)$$

where $dn(\omega, x)/dE = \sum_\alpha dn_\alpha(\omega, x)/dE$, and the frequency-dependent emissivity is defined as

$$\frac{d\bar{n}_\alpha(\omega, x)}{dE} = \int \frac{dE}{2\pi} \frac{f - \bar{f}}{\omega} [G_0^a \Gamma_\alpha \bar{G}_0^r]_{xx}, \quad (9)$$

which is equal to the injectivity in the absence of magnetic field and spin-orbit interaction.

Eq.(8) is the expression which is going to be used in our *ab initio* transport calculation. This equation was derived from the microscopic theory, with three approximations, namely, the wide-band limit, the Thomas-Fermi and the quasi-neutrality. As we can see from Eq.(8), the dynamic conductance is also presented as the conductance of the particle current plus a correction term, structurally very similar to the global formula Eq.(4). The emittance calculation on mesoscopic disordered systems show that qualitatively different behaviors can be obtained for average emittance using two different formulae.²² The following analysis and the calculations in Sec. III will further illustrate how different the results can be from these two formulae.

C. AC emittance

In the low frequency limit, the dynamic conductance can be expanded in terms of frequency ω as following:²³

$$G_{\alpha\beta}(\omega) = G_{0,\alpha\beta} - i\omega E_{\alpha\beta} + \omega^2 K_{\alpha\beta} + O(\omega^3), \quad (10)$$

where $G_{0,\alpha\beta}$ is the dc conductance; $E_{\alpha\beta}$ is called the emittance which characterizes the phase difference between the current and voltage at low frequency;²⁴ $K_{\alpha\beta}$ describes the low frequency dynamic dissipation.

Before further discussions, we note that there is a sign difference between Eq.(1) and the one derived by Büttiker,¹³ where the particle conductance was called the equilibrium admittance. This can be checked by using the Fisher-Lee relation^{25,26} $s(E) = -I + i\sqrt{\Gamma}G^r(E)\sqrt{\Gamma}$. The sign difference is due to definitions of the direction of *positive current*. In all the previous equations, the current I_α in the lead α is defined as the rate of change of the charge in the lead, which is the same as that of Datta²¹ while differs by a sign from that of Büttiker.¹³ However, in the following parts of our paper where we discuss the response of the system due to the external bias especially the imaginary part of the dynamic conductance, we shall adopt the definition of Büttiker for the capacitive-like or inductive-like responses.

Expanding the particle conductance to the first order of ω , we obtain the corresponding emittance,

$$E_{\alpha\beta}^c = \text{Tr} \left[\frac{dn_{\alpha\beta}}{dE} \right], \quad (11)$$

where $dn_{\alpha\beta}/dE$ is the partial density of states defined as²⁷

$$\frac{dn_{\alpha\beta}}{dE} = \frac{1}{2\pi} \text{Re}(\delta_{\alpha\beta} G^r \Gamma_\alpha G^r + i G^r \Gamma_\beta G^a \Gamma_\alpha G^r), \quad (12)$$

the sum of whose second index gives the zero-frequency injectivity, i.e., $\sum_\beta dn_{\alpha\beta}/dE = dn_\alpha/dE$.

The emittance of the atomic systems given by the global formula Eq.(4) is

$$E_{\alpha\beta}^{\text{global}} = E_{\alpha\beta}^c - \frac{\text{Tr}[d\bar{n}_\alpha/dE] \text{Tr}[dn_\beta/dE]}{\text{Tr}[dn/dE]}, \quad (13)$$

where $dn/dE = \sum_{\alpha} dn_{\alpha}/dE$ is the total local density of states, while the emittance derived from the local formula Eq.(8) has the form

$$E_{\alpha\beta}^{local} = E_{\alpha\beta}^c - \text{Tr} \left[\frac{(d\bar{n}_{\alpha}/dE)_{xx} (dn_{\beta}/dE)_{xx}}{(dn/dE)_{xx}} \right]. \quad (14)$$

Eq.(13) and Eq.(14) look very similar, especially in the case when there is no magnetic field or spin-orbit coupling so that $d\bar{n}_{\alpha}/dE = dn_{\alpha}/dE$.

As we can see, the emittance takes the form of the particle emittance minus a correction term due to Coulomb interaction which is positive definite. For the two-probe systems, where α, β can only take L (left) or R (right), and $dn/dE = dn_L/dE + dn_R/dE$, the physical meaning of the emittance can be understood by using the scattering matrix theory, where the local partial density of states (LPDOS) at zero temperature can be well estimated by⁹

$$\text{Tr} \left[\frac{dn_{\alpha\beta}}{dE} \right] = \frac{1}{4\pi i} \text{Tr} \left[s_{\alpha\beta}^{\dagger}(E) \frac{ds_{\alpha\beta}(E)}{dE} - c.c. \right]. \quad (15)$$

Now we consider the case $\alpha = L$ and $\beta = R$. If the system is non-transmissive, then $|s_{LR}|$ and hence $\text{Tr}[dn_{LR}/dE]$ is nearly zero giving rise to a negative emittance E_{LR} due to the correction part. In another word, E_{LL} is positive showing a capacitive-like dynamic response. On the other hand, if the system is highly transmissive such that s_{LL} is nearly zero we have $\text{Tr}[dn_{LL}/dE]$ is negative again due to the correction term. In this case, dynamical response of the system is inductive-like.²⁴

Here for two-probe systems without magnetic field or spin-orbit coupling, we show that there is an inequity between the global emittance and the local one. Now we concentrate on the LR component of both emittance, and their difference is

$$E_{LR}^{local} - E_{LR}^{global} = \frac{\text{Tr}[dn_L/dE] \text{Tr}[dn_R/dE]}{\text{Tr}[dn/dE]} - \text{Tr} \left[\frac{(dn_L/dE)_{xx} (dn_R/dE)_{xx}}{(dn/dE)_{xx}} \right].$$

Using the fact that $(dn_{\alpha}/dE)_{xx}$ are all real non-negative numbers, we can show the difference is always non-negative. To simplify the notation, we denote $a(x) = (dn_L/dE)_{xx}$ and $b(x) = (dn_R/dE)_{xx}$, then what we have to prove is

$$\int a dx \int b dx - \int \frac{ab}{a+b} dx \int (a+b) dx \geq 0.$$

By using $ab/(a+b) = a - a^2/(a+b)$, the left hand side of the above equation can be rearranged as $\int (a+b) dx \int a^2/(a+b) dx - (\int a dx)^2$, which is obviously non-negative due to the Cauchy-Schwartz inequality²⁸ $|\int f(x)g(x) dx|^2 \leq \int |f(x)|^2 dx \int |g(x)|^2 dx$. Hence E_{LR}^{local} is always greater than or equal to E_{LR}^{global} , other components for the emittance hold the same or the opposite inequity due to $E_{LL} = -E_{LR} = -E_{RL} = E_{RR}$, e.g., $E_{LL}^{local} \leq E_{LL}^{global}$. Incidentally, the inequity reduces to an equality if and only if $dn_L/dE = dn_R/dE$ everywhere in space, which hardly happens.

III. NUMERICAL RESULTS

In this section, we calculate the dynamic conductance, especially the emittance for some atomic structures, using both the global formula Eq.(4) and (13) and the local formula Eq.(8) and (14). First we benchmark the results for the Al-C_n-Al system, then we concentrate on the Al-BDT-Al system. We use the state-of-the-art first-principles quantum transport package MATDICAL^{29,30} where DFT is carried out within the formalism of the Keldysh non-equilibrium Green's function, and a linear combination of the atomic orbitals (LCAO) basis set³¹ is employed to numerically solve the Kohn-Sham (KS) equations. The exchange-correlation interaction is treated at the LDA level and a nonlocal norm conserving pseudo-potential³² is used to define the atomic core. The Hamiltonian of the atomic-structure system is determined by DFT, and the non-equilibrium transport properties are determined by NEGF. Real space numerical techniques are used in our calculation, and the NEGF-DFT self-consistent is carried out until the numerical tolerance is less than 10^{-4} .

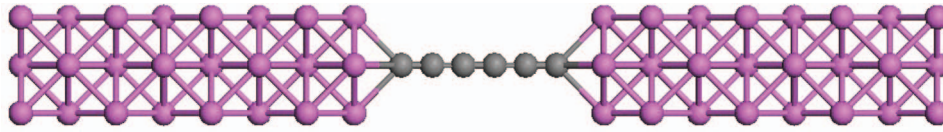


FIG. 1. The schematic structure of Al-C₆-Al system. An atomic wire with six carbon atoms (gray) is sandwiched between two semi-infinite atomic Al electrodes (pink). The Al electrodes extended to $\pm\infty$ along (100) direction.

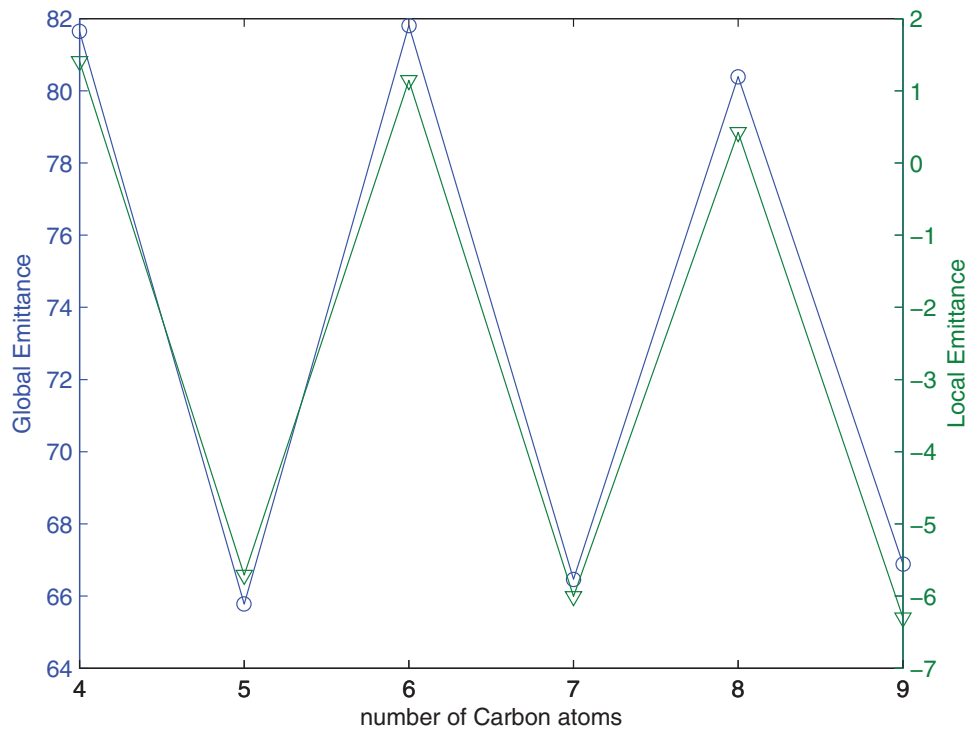


FIG. 2. The LL component of emittance calculated by both the global formula and the local formula for the Al-C_n-Al system, $n = 4, 5, \dots, 9$. The simulation box includes the carbon chain and 16 layers of buffering aluminum. In the figure, the 'global emittance' which means the emittance calculated by the global formula is plotted in blue, while the 'local emittance,' the emittance calculated by the local formula is plotted in green.

A. Benchmark calculation for the Al-C_n-Al system

Up to now, the only ac calculation using MATDCAL is done by Wang *et al.*,¹⁷ using the global formula for the dynamic conductance, where they found that the dynamic conductance exhibits an oscillatory behavior as the number of carbon atoms varies. In this subsection, we calculate the emittance given by the global and the local formulae, not only to show their differences, but also to check whether the emittance given by the local formula also has such an oscillatory behavior.

The Al-C_n-Al structure is depicted in Fig.(1). Here we restate the parameters used in the calculation.¹⁷ The number of carbon atoms varies from four to nine while the configuration of Al atomic electrodes is fixed that the distance of the neighboring aluminum layer is 3.826 a.u.. The distance between the neighboring carbon atom is 2.5 a.u. while the distance between the end carbon atom and the Al electrode is 3.78 a.u.. The scattering region has been chosen as the carbon chain plus 16 buffer layers of aluminum, each side 8 layers. In our calculation, we always assume small bias and small frequency, neglecting the structure deformation caused by ac current.

The calculated results for the emittance are shown in Fig.(2). What we have calculated is the LL component of the emittance, and other components can be trivially obtained. As we can see, the LL component of the emittance calculated from the global formula is much larger than that from the local formula (we have used different vertical axe for results from different formula).

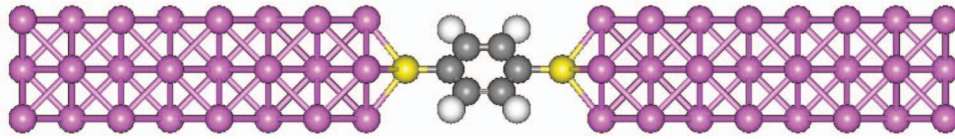


FIG. 3. The schematic structure of Al-BDT-Al system. The leads are two semi-infinite atomic Al electrodes (pink) along (100) direction. In between is a benzenedithiol (BDT) including two sulfur atoms (yellow), four hydrogen atoms (white) and six carbon atoms (carbon). The 2D-structure BDT lies in the (110) plane of the aluminum.

From this figure several observations are in order. First of all, the value of E_{LL} calculated from the local formula is always smaller than of global formula as expected from the inequality we derived. Secondly, the local formula also gives an oscillatory behavior for the emittance as the number of carbon atoms N varies similar to the results obtained from the global formula. Thirdly, it is interesting to note that the local formula predicts a sign change for the emittance when the number of carbon atoms N is odd. Therefore the emittance E_{LL} is positive (the system responds capacitively-like) when N is even, while when N is odd it becomes negative (the response is inductive-like). However, the results from the global formula show that the system gives capacitively-like response regardless of parity of N .

Here we point out that the numerically computational costs for using the two formulae are not comparable. In Eq.(13), the *trace* for those LPDOS can be evaluated naturally in the space of atomic orbitals which is very efficient. In Eq.(14), however, we have to calculate the emissivity or the injectivity at every point in the real space. In order to do so, we have to use the detailed information of those atomic orbitals to perform a projection from the orbital space to the real space, which is very time consuming and is the bottleneck of calculation.

To summarize the benchmark calculation in this subsection, we have shown comparing with the emittance evaluated from the global formula for the Al-C_n-Al system, the emittance calculated by the local formula gives a similar oscillatory behavior as the number of carbon atoms varies, but the values and the computational costs are quite different.

B. Al-BDT-Al system

Taking the benzenedithiol (BDT) as the scattering center, the conductance of gold-benzenedithiol(BDT)-gold molecular junctions has been extensively studied since 1997³³ and the simulation has been done by Ning *et al.*³⁴ which all focused on dc properties. In this subsection, we systematically study the ac conductance and the ac emittance for the system in which the scattering center is BDT but the leads are replaced by aluminum for simplicity.

Fig.(3) depicts the schematic Al-BDT-Al structure that we considered. The system parameters are listed below. The aluminum electrodes are extended along (100) direction and the distance of the neighboring layer is 3.826 a.u., as same as in Al-C_n-Al. The BDT lies in the (110) plane of the aluminum, and its structure comes from the experiment.³⁵ The distance from the aluminum electrode to the edged sulfur atom is 3.056 a.u.. In our calculation, like before, 16 aluminum buffer layers have been included in the scattering region, each side having 8 layers.

For this structure, firstly, we calculate both the dynamic conductance Eq.(4) and (8), and their corresponding emittance Eq.(13) and (14). The imaginary part of the dynamic conductance $\text{Im}[G_{LL}(\omega)]$ are compared with $-\omega E_{LL}$ in the frequency domain from 0 to 50THz in Fig.(4). Although it is known that it may be difficult to check the results experimentally when the frequency approaches to 10THz,¹⁷ the imaginary part of the dynamical conductance seems to be fully contributed by the emittance up to 50THz for both the global and the local formulae. In spite of the linear behavior of $\text{Im}[G_{LL}(\omega)]$, we also see that E_{LL} calculated by the global formula is two orders of magnitude larger than that from the local formula, explicitly, $E_{LL}^{global} = 93.88$ and $E_{LL}^{local} = 0.6929$.

The real part of the dynamic conductances $\text{Re}[G_{LL}(\omega)]$ are also calculated, shown in Fig.(5). When the frequency goes to zero, both $\text{Re}[G_{LL}^{global}(\omega)]$ and $\text{Re}[G_{LL}^{local}(\omega)]$ approach to the same dc value which comes from the particle current only. Using the binomial fitting, the parameter K_{LL}

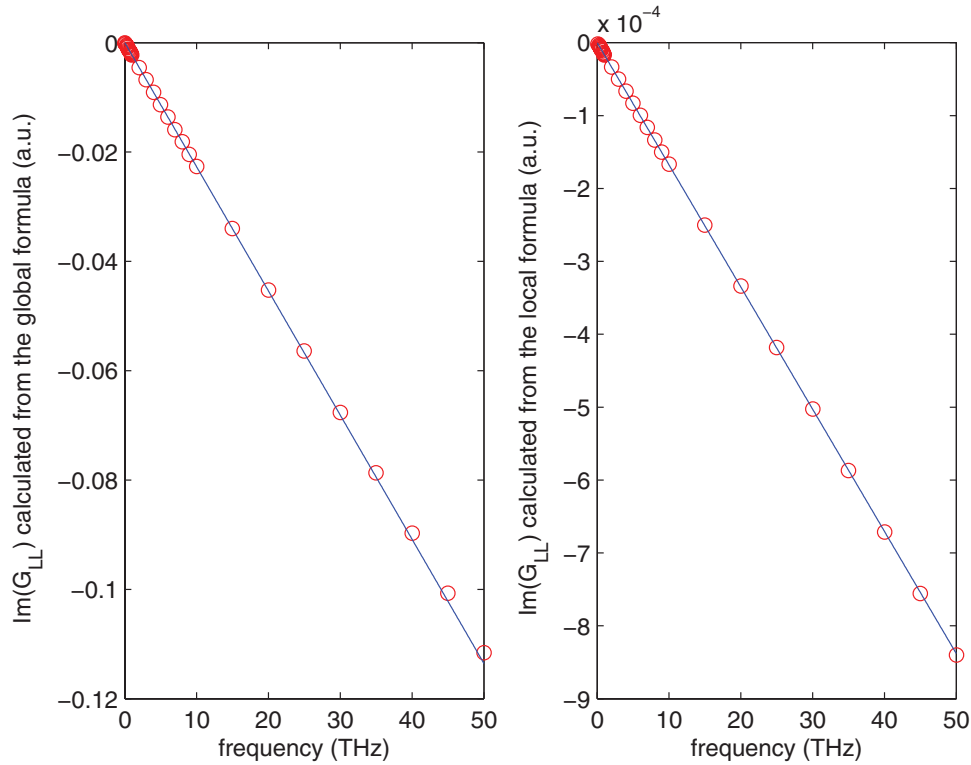


FIG. 4. The imaginary part of the LL component of the dynamic conductance $\text{Im}[G_{LL}(\omega)]$ calculated by either the global or the local formula (red dots), comparing with $-\omega E_{LL}$ (blue lines) from 0 to 50THz. The linear behavior of the imaginary part of the dynamic conductance even holds up to 50THz, and the slope is none other than the negative of its corresponding emittance.

defined in Eq.(10) can be found as $K_{LL}^{global} = 8.776 \times 10^3 a.u.$ and $K_{LL}^{local} = 79.54 a.u.$, and other components are trivially obtained from $K_{LL} = -K_{LR} = -K_{RL} = K_{RR}$. We see that the absolute value of $K_{\alpha\beta}$ calculated from the global formula is also about two orders of magnitude larger than that calculated from the local formula, just like the emittance, showing that the local formula predicts a slower varying of both the imaginary and the real part of the dynamic conductance as the frequency increases from zero.

Now getting back to the ac emittance, we study the behavior of the emittance as when the Fermi level shifts. Numerically, if the Fermi level is shifted by ΔE , what we only have to do is to change $f = f(E - E_f)$ to $f = f(E - E_f - \Delta E)$ in every formula related to f and \bar{f} . The results are shown in Fig.(6), which can be analyzed with the help of the inset of Fig.(6) depicting $\text{Tr}[dn/dE]$ as a function of ΔE . As we can see from the figure, the emittance given from the global formula has similar behavior as the total density of states while the local result does not.

IV. SIZE EFFECT

This section is devoted to what we call *size effect* of the numerical results, which may be first noticed by Büttiker.²³ In the theoretical view, this effect seems trivial, but it worths noticing for both the computational and the experimental physicists.

The origin of the ‘size effect’ for the emittance comes from the fact that the Coulomb interaction is considered only in the scattering region. Specifically, to compute emittance we have to evaluate a *trace* over quantities related to the LPDOS. Theoretically, one can assume that the *trace* over the space containing the scattering center only (e.g. the BDT in the Al-BDT-Al system), but there exists a subtle difference when one performs an *ab initio* transport calculation. Actually, in the *ab initio* calculation for a two-probe atomic-wire structure, the effect of semi-infinite electrodes is accounted

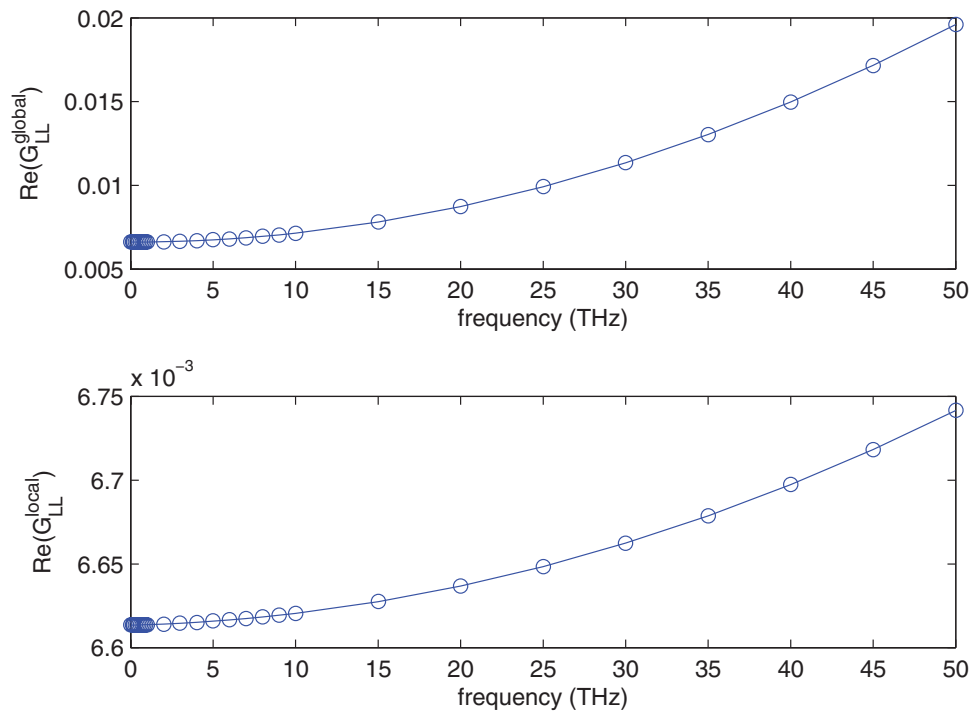


FIG. 5. The real part of the LL component of the dynamic conductance $\text{Re}[G_{LL}(\omega)]$ (a.u.) calculated by either the global or the local formula. The frequency domain ranges from 0 to 50THz. Both of the curves show a binomial behavior, with a vanishing slope near zero frequency. $\text{Re}[G_{LL}^{\text{global}}(\omega)]$ varies faster than $\text{Re}[G_{LL}^{\text{local}}(\omega)]$ as the frequency increases.

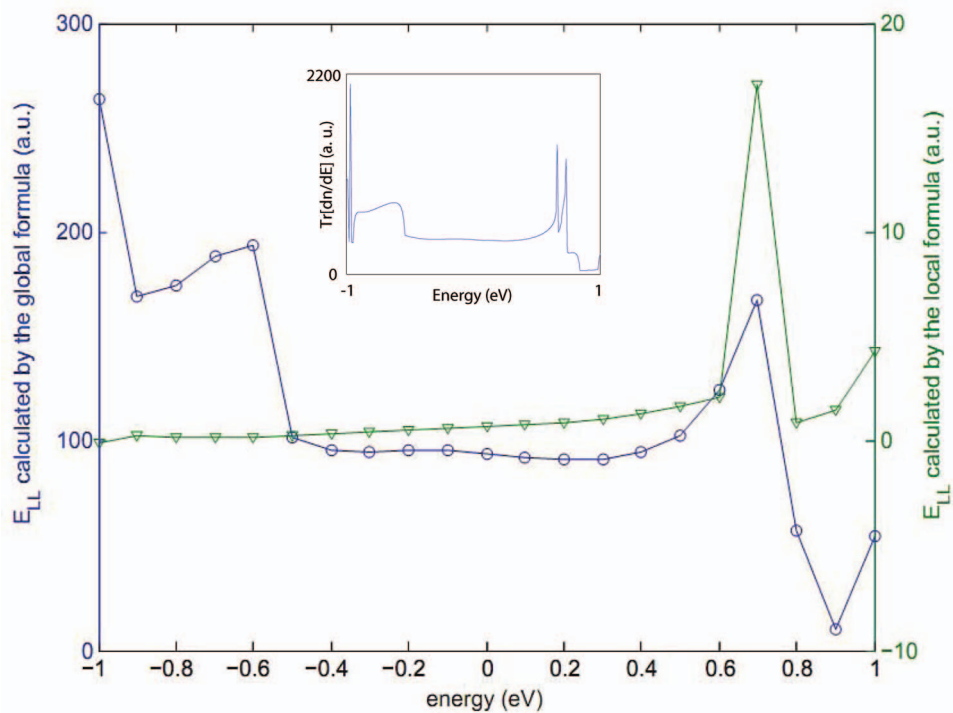


FIG. 6. The LL component of emittance calculated by both the global formula (blue dots) and the local formula (green triangles) for the Al-BDT-Al system, against the shifted Fermi level from -1eV to 1eV. The inset is the global total density of states as a function of the shift of the Fermi level, which behaves more similarly to the global result than to the local result.

for by the self-energy. However, part of the electrode (the buffer layer) has to be included in the scattering region. These buffer layers are used to screen the effect of scattering center such that at the boundary of the scattering region, both the Coulomb potential and the wave function can smoothly match those of the electrodes. This is so called screening approximation in NEGF+DFT scheme. After convergence, the *trace* is taken over the scattering region rather than the scattering center. If we only calculate the dc properties of a system, the trace over the scattering region and that over the scattering center should not affect the transmission coefficient which is the most important physical quantity in dc case, because the static Coulomb interaction has been included both in the scattering center as well as in the electrodes. However, when one calculates the ac conductance and traces over different sizes, the results could be different — that is why we always address how many buffer layers have been included in the scattering region in the previous sections. As an example, for the result of the Al-C_n-Al system shown in Fig.(2), the global results simply reproduce Wang's work,¹⁷ but the values of the emittance will change drastically as the number of buffer layers is increased or decreased. This is because the emittance describes the phase between current and voltage. In general, emittance can give capacitive-like behavior or inductive-like behavior depending whether the system is transmissive or not. If more buffer layers are added in the simulation box, the electron will accumulate more phase. As a result, kinetic inductance of the device increases and this in turn affects the emittance.

For the Al-BDT-Al system, we investigate the numerical results as the size varies, beginning from dc case, which can be viewed as the zero-frequency limit of ac case. From either Eq.(4) or Eq.(8), we have

$$G_{\alpha\beta}^{dc} = \frac{1}{2\pi} \text{Tr}[G_0^r \Gamma_\beta G_0^a \Gamma_\alpha - G_0^r \Gamma G_0^a \Gamma_\alpha \delta_{\alpha\beta}]. \quad (16)$$

In a two probe system, we have $G_{LR}^{dc} = 1/(2\pi)T_{LR}$, where T is the transmission function defined as $T_{\alpha\beta} = \text{Tr}[\Gamma_\alpha G_0^r \Gamma_\beta G_0^a]$ calculated at the Fermi level. In Fig.(7), we plot the transmission function T_{LR} for the Al-BDT-Al system as the function of the shifted Fermi level for different numbers of buffer layers included in the scattering region. The collapse of these lines show that the 'size effect' does not affect the transmission function at all, even if the Fermi level is shifted.

However, the situation becomes very different if we calculate the emittance, shown in Fig.(8) where both the global formula and the local formula are used. The 'size effect' is clearly exhibited in this figure. Besides, the behaviors of the calculated emittance from two formulae versus the number of the buffer layers are also different. As we can see from the figure, as the number of buffer layers varies, E_{LL} calculated from both formulae remain positive. However, the global formula seems to predict an increasing behavior for E_{LL} as the number of buffer layers increases while the result given by the local formula seems to give an oscillatory behavior with the amplitude decreasing. It is interesting to ask whether the value of E_{LL}^{local} will change sign if when number of buffer layers included in the scattering region becomes very large. This question is difficult to answer for the real atomic system. Numerically, the calculation suffers from both the computational time and the convergence problem as the scattering region becomes large. Physically, we know that there are seven transverse modes in the aluminum electrodes, so it is difficult to explain these features. However, we may get some insight from exactly solvable model. To appreciate the 'size effect,' we consider a 1D toy model from the textbook.²⁶

The toy model is a 1D wire (single mode) having two scatterers separated by a distance d , thus the scattering potential is $U(x) = U_0[\delta(x) + \delta(x - d)]$. Numerically, we assume $U_0 = 9\text{eV}\text{\AA}$, $d = 50\text{\AA}$ and the effective mass of the electron is $m = 0.07$, and the 'emittance' is calculated at the energy $E = 0.5\text{eV}$ by both the global and the local formulae. The results are shown in Fig.(9), showing that when the scattering region increases, the emittance shows a generally linear property with periodically oscillations.

Such behavior of the emittance as size varies can be appreciated by using the representation of the scattering matrix. Suppose the scattering matrix of the double-well with no buffer layer is s_0 , so if we include buffer layers with total length by L , both sides of well having $L/2$, the scattering matrix

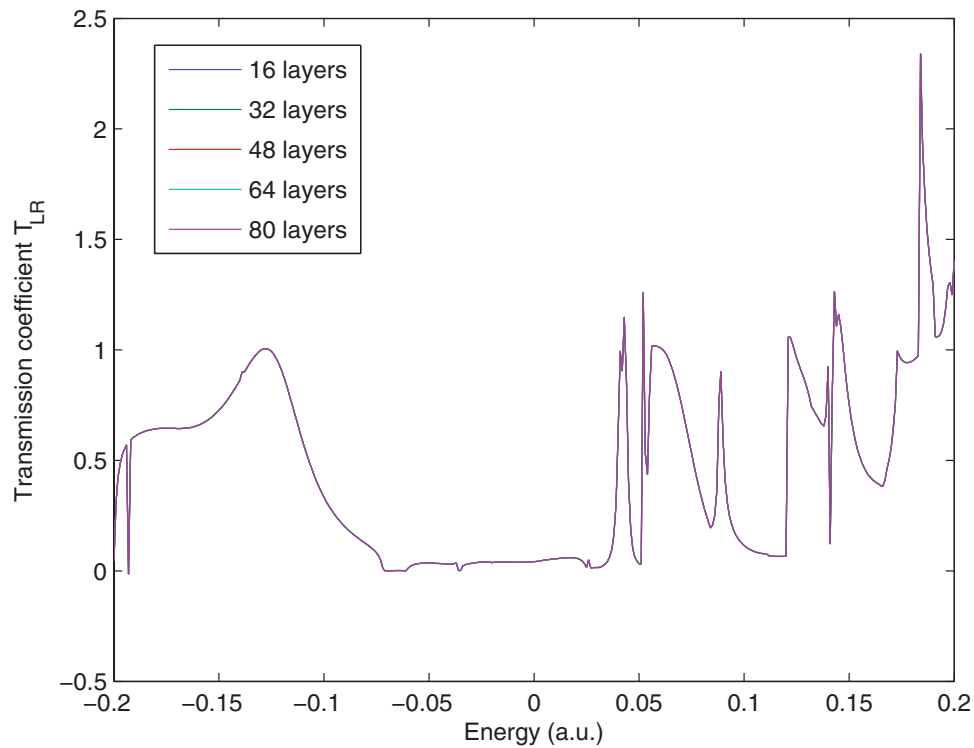


FIG. 7. The transmission function T_{LR} for the Al-BDT-Al system calculated at different energy. There are five lines representing different numbers of buffer layers that are included in the scattering region, and these lines collapse to a single curve.

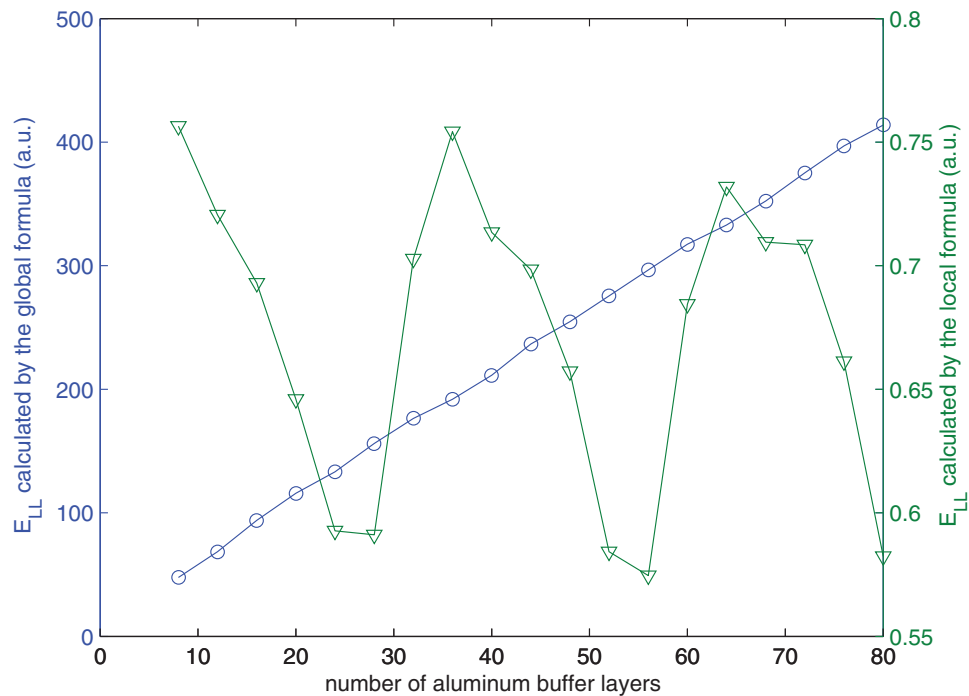


FIG. 8. The LL component of emittance calculated by both the global formula (blue dots) and the local formula (green triangles) for the Al-BDT-Al system, against the number of buffer layers included in simulation box. It seems the one calculated by the global formula shows the generally linear behavior while the one calculated by the local formula shows the oscillatory behavior.

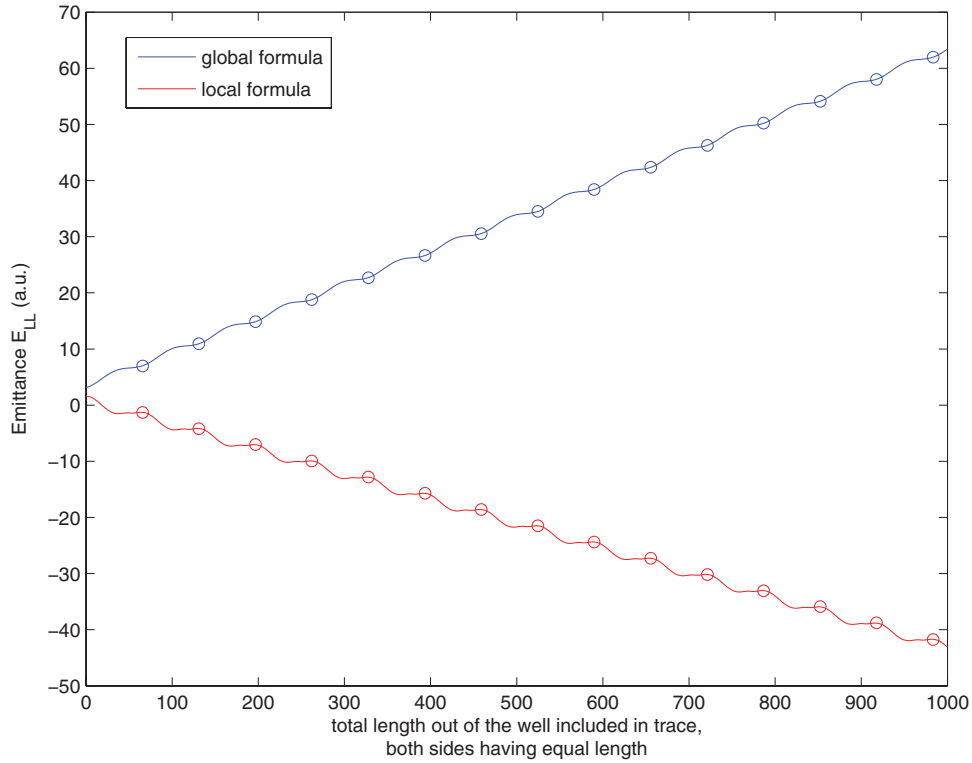


FIG. 9. 1D double-delta-potential-well system, the LL component of the ac emittance calculated against the length of the leads out of the potential well, with both sides having equal length, by the global formula (blue) and the local formula (red) respectively. The figure shows that the emittance calculated by either method has a generally linear with periodically oscillatory property. The period is represented by the circle dots.

becomes

$$s = \begin{bmatrix} 0 & e^{ikL/2} \\ e^{ikL/2} & 0 \end{bmatrix} \otimes s_0 \otimes \begin{bmatrix} 0 & e^{ikL/2} \\ e^{ikL/2} & 0 \end{bmatrix} \quad (17)$$

where $k = \sqrt{2mE}$ is the wave vector and \otimes is the symbol to combine scattering matrices. The transmission function will not be changed because s_{LR} and s_{0LR} only differ by a phase, while $T_{LR} = |s_{LR}|^2$. However, if we consider the emittance Eq.(13) or Eq.(14), we find that the emittance is closely related to the LPDOS, hence the behavior of the LPDOS will determine the behavior of the emittance. From Eq.(15), we see that the LPDOS given by s_0 and s should be different. The general linear behavior of the emittance comes from the derivative that $\partial_E e^{ikL/2} \sim \frac{1}{2} ikL e^{ikL/2}/m$, and the period of the oscillation is $2\pi/k = 65.555\text{\AA}$, shown in Fig.(9). Besides, the local formula Eq.(14) implies an additive property for the length of extension. In our 1D model, if the length of extension is increased by one period (i.e., each side extends by a half period), it contributes to E_{LR}^{local} by a constant, which is about $-2.7432a.u.$. This constant is determined by the energy at which the emittance is calculated and the potential profile of both the ‘lead’ and the scattering center. We note that this additive property for the local formula also holds for the realistic system, but similar arguments can not be made for the global formula. To summarize the ‘size effect,’ we have shown that this effect comes from the kinetic inductance. This effect does not affect the dc transmission function but critically affects the ac emittance.

V. CONCLUSION

In this paper, we have investigated the dynamical conductance of atomic junctions from first principles using NEGF+DFT method. We have used the expression of dynamical conductance

derived from microscopic theory that explicitly includes Coulomb interaction (local formula). In particular, we have calculated the dynamical conductance as well as emittance for the Al-C_n-Al and the Al-BDT-Al atomic systems. As a benchmark calculation, we have also calculated the emittance using phenomenological theory using current partition (global formula). For both Al-C_n-Al and Al-BDT-Al systems, our results show that the global formula overestimate the emittance by almost two orders of magnitude. Both global and local formulae give the same oscillatory behavior when the number of carbon chain *N* changes from odd to even. However, the microscopic theory predicts different response when *N* is odd (inductive-like) or even (capacitive-like) while the results of phenomenological theory give capacitive-like response for all carbon chains. Since the emittance characterize the phase accumulated in the scattering region, its value depends on the system size or the buffer layers of the leads which contributes via kinetic inductance. Finally, we emphasize that although a better theory (microscopic theory) is available to calculate the ac conductance of atomic systems the calculation is very costly due to the fact that it has to be performed in real space.

ACKNOWLEDGMENTS

The authors would like to thank B. Wang, Y. Wang, Y. X. Xing, F. Xu and H. Y. Yu for helpful discussions. We gratefully acknowledge the support from Research Grant Council (HKU 705409P) and University Grant Council (Contract No. AoE/P-04/08) of the Government of HKSAR.

- ¹T. H. Oosterkamp, L. P. Kouwenhoven, A. E. A. Koolen, N. C. van der Vaart, and C. J. P. M. Harmans, *Phys. Rev. Lett.* **78**, 1536 (1997), T. H. Oosterkamp, T. Fujisawa, W. G. van der Wiel, K. Ishibashi, R. V. Hijman, S. Tarucha, and L. P. Kouwenhoven, *Nature (London)* **395**, 873 (1998).
- ²G. B. Lesovik and L. S. Levitov, *Phys. Rev. Lett.* **72**, 538 (1994).
- ³C. Bruder and H. Schoeller, *Phys. Rev. Lett.* **72**, 1076 (1994).
- ⁴A. P. Jauho, N. S. Wingreen, and Y. Meir, *Phys. Rev. B* **50**, 5528 (1994).
- ⁵A. Schiller and S. Hershfield, *Phys. Rev. Lett.* **77**, 1821 (1996).
- ⁶J. C. Cuevas, A. Martin-Rodero, and A. Levy Yeyati, *Phys. Rev. B* **54**, 7366 (1996).
- ⁷R. J. Schoelkopf, A. A. Kozhevnikov, D. E. Prober, and M. J. Rooks, *Phys. Rev. Lett.* **80**, 2437 (1998).
- ⁸Q. F. Sun, J. Wang and T. H. Lin, *Phys. Rev. B* **61**, 12643 (2000).
- ⁹M. Büttiker, *J. Phys.: Condens. Matter* **5**, 9361 (1993).
- ¹⁰S. E. Nigg, R. Lopez, and M. Büttiker, *Phys. Rev. Lett.* **97**, 206804 (2006).
- ¹¹J. Gabelli, G. Feve, J. M. Berroir, B. Placais, A. Cavanna, B. Etienne, Y. Jin, and D. C. Glattli, *Science* **313**, 499 (2006).
- ¹²J. Wang, B. Wang, and H. Guo, *Phys. Rev. B* **75**, 155336 (2007).
- ¹³M. Büttiker, A. Pretre, and H. Thomas, *Phys. Rev. Lett.* **70**, 4114 (1993).
- ¹⁴B. Wang, J. Wang and H. Guo, *Phys. Rev. Lett.* **82**, 398 (1999).
- ¹⁵J. Wu, B. Wang, J. Wang, and H. Guo, *Phys. Rev. B* **72**, 195324 (2005).
- ¹⁶Y. Yu, B. Wang and Y. Wei, *J. Chem. Phys.* **127**, 169901 (2007).
- ¹⁷B. Wang, Y. Yu, L. Zhang, and J. Wang, *Phys. Rev. B* **79**, 155117 (2009).
- ¹⁸Y. Wei and J. Wang, *Phys. Rev. B* **79**, 195315 (2009).
- ¹⁹Z. S. Ma, J. Wang and H. Guo, *Phys. Rev. B* **57**, 9108 (1998).
- ²⁰J. Taylor, H. Guo, and J. Wang, *Phys. Rev. B* **63**, 245407 (2001); *ibid.* **63** 121104 (2001).
- ²¹M. P. Anantram and S. Datta, *Phys. Rev. B* **51**, 7632 (1995).
- ²²W. Ren, F. Xu, J. Wang, *Nanotechnology* **19**, 435402 (2008).
- ²³M. Büttiker and T. Christen, in *Quantum Transport in Semiconductor Submicron Structures*, edited by B. Kramer (Kluwer Academic Publishers, Dordrecht, 1996).
- ²⁴M. Büttiker and T. Christen, in *Mesoscopic Electron Transport*, edited by L. L. Sohn. *et al.* (Kluwer, Dordrecht, 1997).
- ²⁵D. S. Fisher and P. A. Lee, *Phys. Rev. B* **23**, 6851 (1981).
- ²⁶S. Datta, *Electronic Transport in Mesoscopic Systems* (Cambridge University Press, Cambridge).
- ²⁷T. Gramschpacher and M. Büttiker, *Phys. Rev.* **56**, 13026 (1997).
- ²⁸J. Micheal Steele, in *The Cauchy-Schwartz Master Class: an Introduction to the Art of Mathematical Inequalities*, Ch. 1.
- ²⁹D. Waldron, P. Haney, B. Larade, A. MacDonald, and H. Guo, *Phys. Rev. Lett.* **96**, 166804 (2006).
- ³⁰D. Waldron, V. Timoshevskii, Y. Hu, K. Xia, and H. Guo, *Phys. Rev. Lett.* **97**, 226802 (2006).
- ³¹P. Ordejon, E. Artacho, and J. M. Soler, *Phys. Rev. B* **53**, R10441 (1996); J. M. Soler, E. Artacho, J. D. Gale, A. Garcia, J. Junquera, P. Ordejon, and D. Sanchez-Portal, *J. Phys.: Condens. Matter* **14**, 2745 (2002).
- ³²N. Troullier and J. L. Martins, *Phys. Rev. B* **43**, 1993 (1991).
- ³³M. A. Reed, C. Zhou, C. J. Muller, T. P. Burgin, and J. M. Tour, *Science* **278**, 252 (1997).
- ³⁴Z. Ning, W. Ji, H. Guo, arXiv:0907.4674v2 (2009).
- ³⁵H. Song *et al.*, *Nature*, **462**, 1039 (2009).